

Original
Article

Changes in Internal Thoracic Artery Blood Flow According to the Degree of Stenosis of the Anterior Descending Branch of the Left Coronary Artery

Ken Nakamura,¹ Mitsutaka Nakao,² Makoto Wakatabe,² Kouan Orii,² Takatomo Nakajima,³ Shohei Miyazaki,⁴ and Takashi Kunihara¹

Purpose: Computational fluid dynamics has enabled the evaluation of coronary flow reserve. The purpose of this study was to clarify the hemodynamic variation and reserve potential of the left internal thoracic artery (LITA).

Methods: Four patients were selected on the basis of various native coronary stenosis patterns and graft design. The wall shear stress and oscillatory shear index were measured, and one patient was selected. Next, we created three hypothetical lesions with 75%, 90%, and 99% stenosis in front of the graft anastomosis, and compared the changes in LITA blood flow and coronary flow distribution.

Results: In the 75% to 90% stenosis model, blood flow was significantly higher in the native coronary flow proximal to the coronary artery bypass anastomosis regardless of time phase. In the 99% stenosis model, blood flow from the LITA was significantly dominant compared to native coronary flow at the proximal site of anastomosis. The range of LITA flow variability was the largest at 99% stenosis, with a difference of 70 ml/min.

Conclusion: The 99% stenosis model showed the highest LITA flow. The range of LITA flow variability is large, suggesting that it may vary according to the rate of native coronary stenosis.

Keywords: wall shear stress, oscillatory shear index, reserve potential of LITA

¹Department of Cardiac Surgery, The Jikei University School of Medicine, Tokyo, Japan

²Department of Cardiac Surgery, Saitama Cardiovascular and Respiratory Center, Kumagaya, Saitama, Japan

³Department of Cardiology, Saitama Cardiovascular and Respiratory Center, Kumagaya, Saitama, Japan

⁴Cardio Flow Design Inc., Tokyo, Japan

Received: August 24, 2022; Accepted: October 31, 2022

Corresponding author: Ken Nakamura. Department of Cardiac Surgery, The Jikei University School of Medicine, 3-25-8, Nishi-shinbashi, Minato-ku, Tokyo 105-8461, Japan
Email: cardiacsurgken@gmail.com



This work is licensed under a Creative Commons Attribution-NonCommercial-NoDerivatives International License.

©2023 The Editorial Committee of *Annals of Thoracic and Cardiovascular Surgery*

Abbreviations and Acronyms

LITA = left internal thoracic artery
LAD = left anterior descending artery
WSS = wall shear stress
OSI = oscillatory shear index
CFD = computational fluid dynamics
CABG = coronary artery bypass grafting
CT = computed tomography
PI = pulsatility index
TTFM = transit-time flow measurement
RITA = right internal thoracic artery

Introduction

The use of the left internal thoracic artery (LITA) for left anterior descending artery (LAD) is the golden standard,

based on large registries in the United States.^{1,2} Blood flow in the LITA is affected by various factors, and changes in blood flow after coronary artery bypass grafting (CABG) vary depending on the timing of measurement.³ There are many factors that regulate internal thoracic artery (ITA) flow, including spasm, anastomotic technical problems, and graft problems,⁴ but ITA flow can also change through regulating the native proximal LAD during surgery.⁵ This is because of competition between the bypass graft flow and the native coronary artery flow, and it has been reported that competitive flow may be the cause of future stenosis in ITA grafts.⁶ Competition for blood flow appears in the form of wall shear stress (WSS) and oscillatory shear index (OSI), which has been reported to affect graft patency.^{7,8}

In recent years, computer flow simulation modeling based on computational fluid dynamics (CFD) has enabled the evaluation of coronary artery blood flow reserve based on fluid dynamics, and many blood flow analyses have been reported.⁹ CFD uses numerical computation to solve and analyze fluid flows. CFD provides flow velocity and pressure distribution at an arbitrary time.⁹ Cardiovascular surgery is a good application for CFD modeling simulation of the change in hemodynamics after surgery.^{9,10}

In this study, we applied this technology during CABG to create a hypothetical coronary artery stenosis lesion model and investigated the hemodynamic behavior of LITA blood flow anastomosed to the LAD according to the degree of stenosis of the native LAD using computer analysis. The purposes of this study were to clarify the hemodynamic variation and reserve potential of LITA according to the native coronary artery stenosis rate and to enable the preoperative simulation of future bypass models.

Patients and Methods

This study was approved by the institutional review board (IRB) of the Saitama Cardiovascular and Respiratory Center (No. 2021009).

Operation and patient characteristics

Patients who underwent CABG performed at our institution between January 2018 and December 2019 by the same surgeon (K.N.) and who consented to this clinical study were included. For LITA–LAD anastomosis, side-to-side anastomosis was performed.

Patients with impaired cardiac function (left ventricle ejection fraction <40%), frequent arrhythmias, and impaired renal function, and patients for whom coronary computed tomography (CT) angiography is not feasible were excluded. Emergency and reoperation cases were

also excluded. All other patients had a coronary angiography CT scan before and after CABG surgery.

In this study, different stenosis models of LAD and graft design models were prepared in order to investigate various coronary blood flow patterns using CFD.

To begin, we selected patients who had good results in the CABG flow measurement of the LITA–LAD as graft design. Patients with a pulsatility index (PI) of less than 3.0 and a blood flow rate of at least 15 ml/min were considered to have good blood flow¹¹ by transit-time flow measurement (TTFM) (Medistim, Oslo, Norway). Four patients were selected from various native coronary stenosis patterns and graft design patterns based on the following criteria.

The conditions were as follows:

- 1) How WSS and OSI work on the native coronary vessel after native coronary stenosis
- 2) Patients with stable OSI proximal to the CABG anastomosis
- 3) ITA blood flow less than PI 3.0 after bypass surgery
- 4) ITA blood flow of 15 ml/min or more

The characteristics of four patients are shown in **Table 1**. The WSS and OSI were measured in these four patients, and one patient with better LITA blood flow and steady WSS and OSI was selected.

Results of patient selection

Case 1 had the second highest ITA blood flow but had a high OSI proximal to the CABG anastomosis. Case 2 had the best ITA blood flow of the four cases. In addition, the OSI after CABG was stable. Case 3 was a right internal thoracic artery (RITA) graft design model, but the WSS of the LAD was high preoperatively, and the OSI after bypass was not as stable as in Cases 1 and 2. Case 4 was also a RITA graft design, but the high native stenosis rate made it unsuitable for case selection. The results of the WSS and OSI of the four patients are shown in **Figs. 1a–1d**.

Based on these results, Case 2 was selected as a model case for virtual stenosis.

Next, we created three hypothetical lesions with 75%, 90%, and 99% stenosis proximal to the graft anastomosis of the LAD in the selected patients, and compared the changes in ITA blood flow and coronary flow distribution in the left coronary artery (LCA) region under each condition (**Fig. 1e**).

CFD

CFD was calculated as the spatiotemporal field of velocity and pressure in the target domain by solving the continuity equations and the Navier–Stokes equations. These equations were solved in a computational mesh,

Table 1 Cases 1 and 2 were LITA models. Case 2 had the best ITA blood flow of the four cases

	LMT	No. 6	No. 7	Graft design to LCA	Graft flow to LAD (ml/min)	PI	Graft flow to Cx (ml/min)	PI	Amount LAD + Cx (ml/min)
Case 1	0%	75%	75%	LITA-LAD	37	1.7	19	1.8	56
Case 2	0%	75%	90%	SVG-HL-PL	46	2	28	3.9	74
Case 3	90%	50%	0%	LITA-LAD	26	2.5	14	1.8	40
Case 4	0%	0%	100%	LITA-OM	27	1.7	25	2.6	52
				RITA-LAD					
				LITA-PL					

LITA: left internal thoracic artery; ITA: internal thoracic artery; PI: pulsatility index; SVG: saphenous vein graft; LCA: left coronary artery; LAD: left anterior descending artery; LMT: left main coronary trunk; OM: obtuse marginal branch; PL: posterolateral branch; D1: diagnosis 1; RITA: right internal thoracic artery; HL: high lateral branch

which divided the volume of the segmented heart and vessel structures into spatially discrete small cells called the computational mesh or grid.⁹⁾ Detailed calculation and analysis were carried out by Cardio Flow Design Inc., Japan. The CFD method was based on prior validation studies. The vessel geometry was created from an enhanced multidetector-row CT using Ziostation (Ziosoft, Tokyo, Japan) and Blender (Blender Foundation, Amsterdam, The Netherlands). Computational meshes were created with ANSYS-ICEM CFD 16.0 (ANSYS Japan, Tokyo, Japan). The inlet boundary condition at the aortic root was 5.0 L/min. The outlet boundary conditions at the neck vessel branches and descending aorta were set as the pressure boundary conditions representing the external forces outside the analysis domain. The physiological external forces in the cervical vessels and the descending aorta were composed of the wave reflection from peripheral tissues, vascular inactivation, and autonomic regulation.

Time-varying impedance boundary conditions were used for the coronary artery outlet boundary conditions to represent ventricular muscle contraction and relaxation. The impedance of coronary branches was estimated from the amount of myocardial perfusion volume of each branch. Blood was assumed to be an incompressible Newtonian fluid with a density of 1060 kg/m³ and a viscosity of 0.004 Pa·s. The Navier–Stokes equations were solved using the fine volume method with the convergence criteria of 1.0 E⁻⁵ for all parameters on the open-source CFD software OpenFOAM (OpenFOAM Foundation: free, open source software; England).⁹⁾

WSS and OSI⁷⁻⁹⁾

CFD was used to measure the WSS and the OSI (the degree to which the direction of WSS changes within a

single beat) of each of the four previously selected patients.

WSS is defined based on the flow velocity profile inside the cardiovascular lumen.

The WSS vector τ is calculated by using the velocity profile around the vessel wall.

How to measure WSS

$$\text{WSS vector } \tau = \mu \partial(\mathbf{u} - (\mathbf{u} \cdot \mathbf{n}_y) \mathbf{n}_y) / \partial y$$

where \mathbf{u} is the flow rate, y is the coordinate system perpendicular to the wall, \mathbf{n}_y is normal to the wall in the y direction, μ is the coefficient of viscosity, and WSS is equal to $\|\tau\|$.

How to measure OSI

$$\text{OSI} = 1/2(1 - \tau^{NM}/\tau^{MN})$$

where NM is norm of the mean and MN is mean of the norm.

If the WSS was within the normal range after CABG anastomosis, it indicated that there was a low likelihood of future anastomotic stenosis.⁹⁾

In this study, we have estimated the stability of the WSS and OSI with a small spatial variation in WSS and a small OSI.

It is often said that too low WSS and high OSI lead to increased plaque, while moderate WSS and low OSI are good for the coronary arteries. In coronary arteries, flow is often disrupted by bifurcation and stenosis. When bypass is used, it is further disrupted by the collision of bypass and native blood flow. In addition, changes in the balance between native and bypass blood flow within a heartbeat can alter the direction of blood flow, leading to a decrease in WSS and an increase in OSI. CFD is useful for analyzing complex phenomena that combine these various factors.

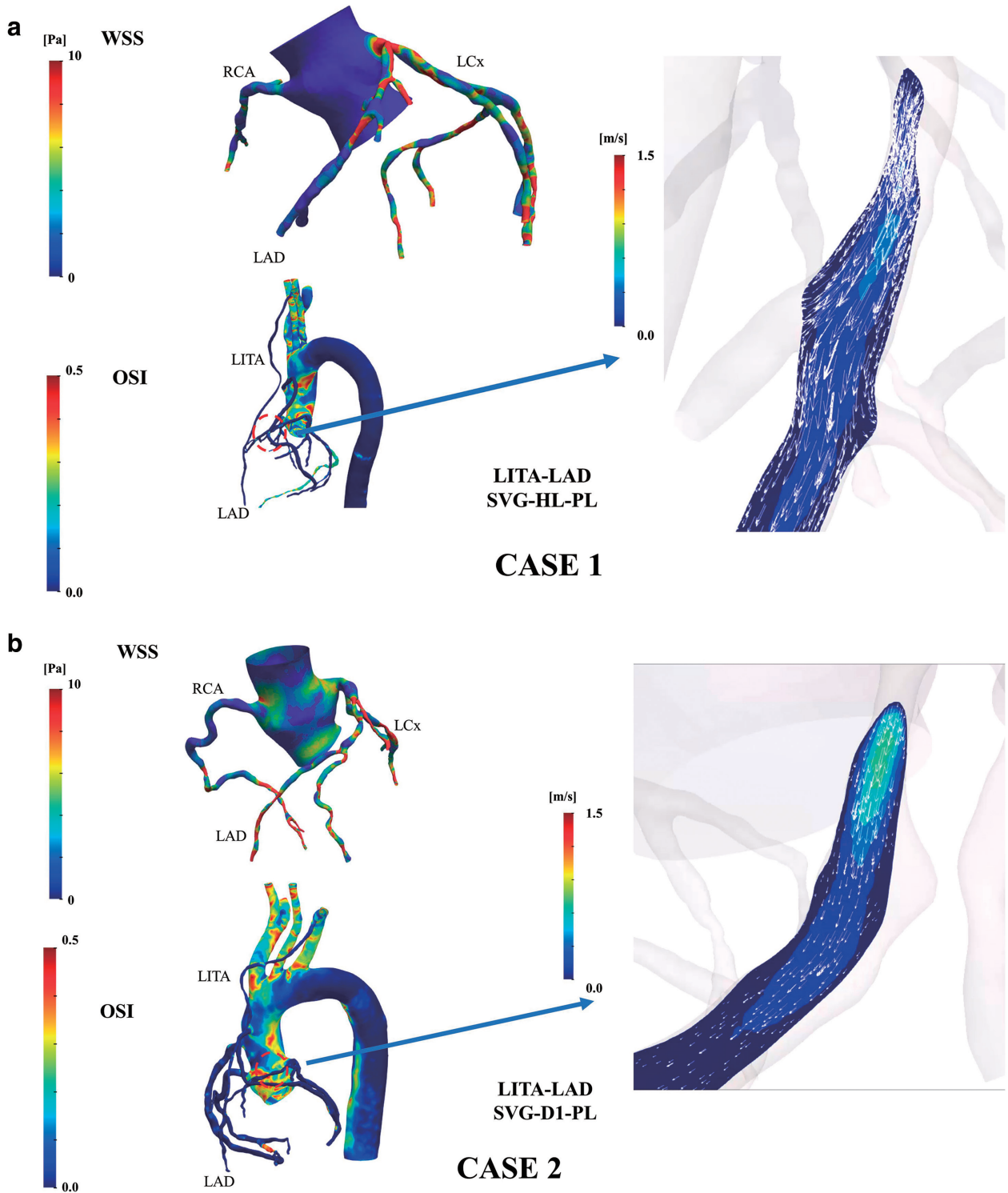


Fig. 1 (Continued)

Results

For Case 2, we created a virtual stenosis at the original No. 6 lesion site and evaluated coronary blood flow. The WSS and OSI are presented in Fig. 2. The

ITA flow rate and streamline are shown in Figs. 3a–3c and Video 1 (the video is available online). A comparison of the average flow rate of each section and the range of variability in LITA blood flow is listed in Table 2.

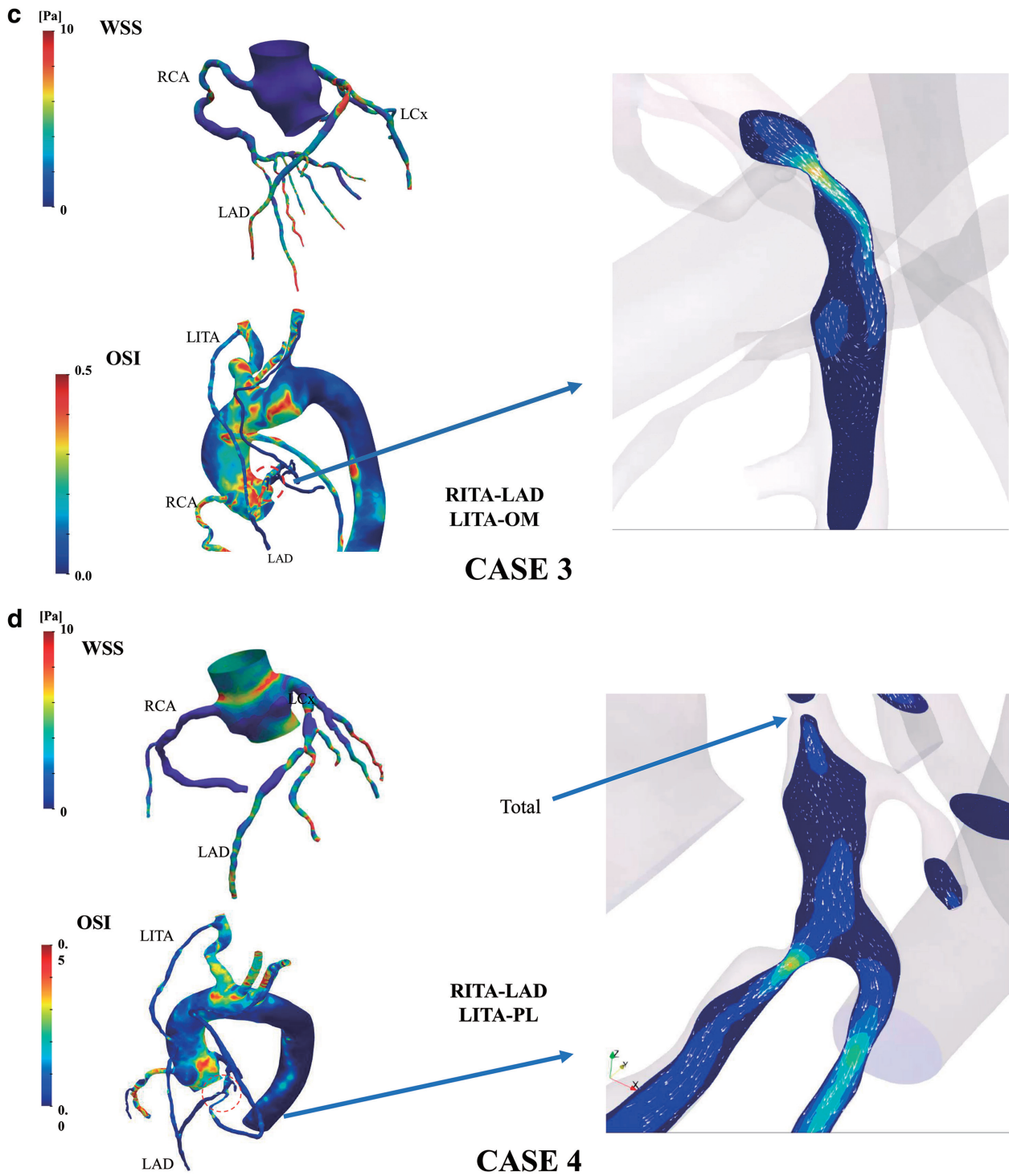


Fig. 1 (Continued)

75% stenosis model (Fig. 3a)

The LITA average flow was 18.9 ml/min, and there was an inverse flow phase at 0.2 s systole. The LAD average flow was 66.9 ml/min and the diagnosis 1 (D1) and diagnosis 2 (D2) average flow were 38.8 ml/min and 12.5 ml/min, respectively. The septal branch (SEP) average flow was 29.6 ml/min.

LITA had a minimum blood flow of -5 ml/min at 0.2 s and a maximum flow rate of 28 ml/min at 0.7 s with a difference of 33 ml/min. The WSS at the LAD anastomosis was the lowest of the other models. The OSI at the LAD anastomosis was the highest of the other models.

e create a hypothetical coronary artery stenosis lesion model

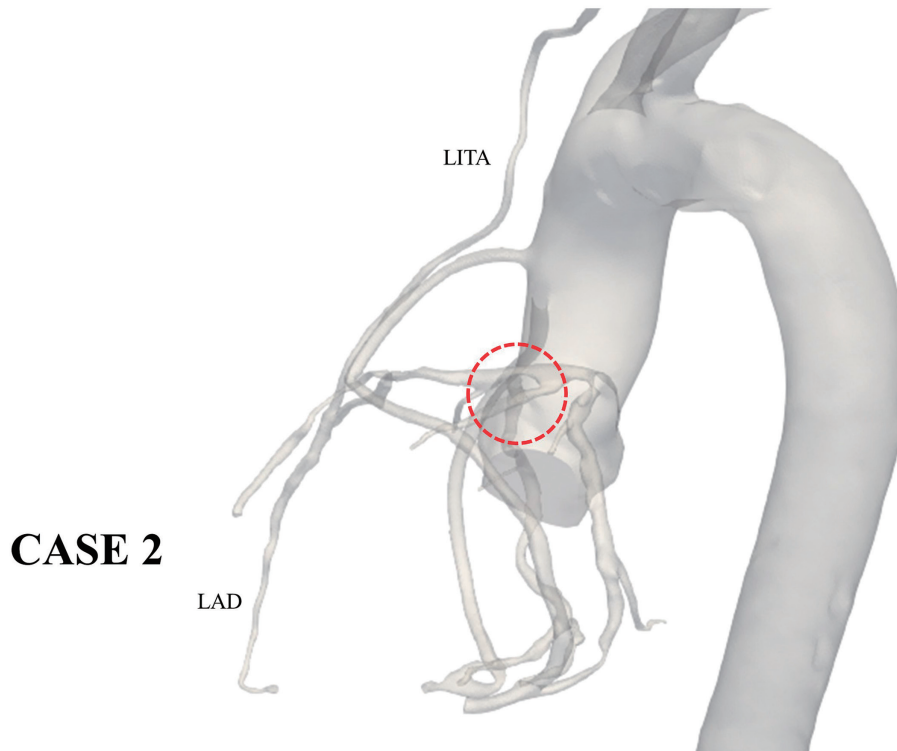


Fig. 1 (a) Case 1: LITA-LAD and SVG-HL-PL. (b) Case 2: LITA-LAD and SVG-D1-PL. (c) Case 3: RITA-LAD and LITA-OM. (d) RITA-LAD and LITA-PL. (e) Creation of a hypothetical coronary artery stenosis lesion model. Case 2 had the best ITA blood flow of the four cases. In addition, the WSS and OSI after CABG were stable. Three hypothetical lesions with 75%, 90%, and 99% stenosis in front of the graft anastomosis of the LAD were created in Case 2. LAD: left anterior descending artery; SVG: saphenous vein graft; HL: high lateral branch; PL: posterolateral branch; OM: obtuse marginal branch; D1: diagnosis 1; LITA: left internal thoracic artery; RITA: right internal thoracic artery; WSS: wall shear stress; OSI: oscillatory shear index; CABG: coronary artery bypass grafting

90% stenosis model (Fig. 3b)

The LITA average flow was 40.4 ml/min and there was no inverse flow in the concurrent phase. The LAD average flow was 62.6 ml/min and the D1 and D2 average flow were 38.9 ml/min and 11.2 ml/min, respectively. The SEP average flow was 26.6 ml/min. LITA had a minimum blood flow of 18 ml/min at 0.15 s and a maximum flow rate of 59 ml/min at 0.7 s with a difference of 41 ml/min. The WSS and OSI at the LAD anastomosis were in the middle of the three models.

99% stenosis model (Fig. 3c)

The LITA average flow rate was 72.9 mL/min and there was no inverse flow in the concurrent phase. The LITA blood flow was reversed immediately before the D1 branch of the native coronary blood flow. The LAD average flow rate was the lowest at 54.4 mL/min, and the D1 and D2 average flow were 39.1 ml/min and 9.1 ml/min, respectively. The SEP average flow was 22.1 ml/min. LITA had a minimum blood flow of 28 ml/min at 0.12 s

and a maximum flow rate of 98 ml/min at 0.7 s with a difference of 70 ml/min.

The WSS at the LAD anastomosis was the highest of the other models. The OSI at the LAD anastomosis was the lowest of the three models.

In the 75% to 90% stenosis model, blood flow was significantly higher in the native coronary flow proximal to the CABG anastomosis regardless of time phase. In the 99% stenosis model, blood flow from the LITA graft was significantly dominant compared to the native coronary flow at the proximal site of anastomosis. D1, D2, and SEP flow were constant regardless of time phase, resulting in a low OSI in all models. The range of LITA flow variability was the largest at 99% stenosis, with a difference of 70 ml/min.

Discussion

The superiority of the ITA for CABG over catheter interventions and over any other graft has been established by the evidence of long-term patency.^{12,13} CFD has been

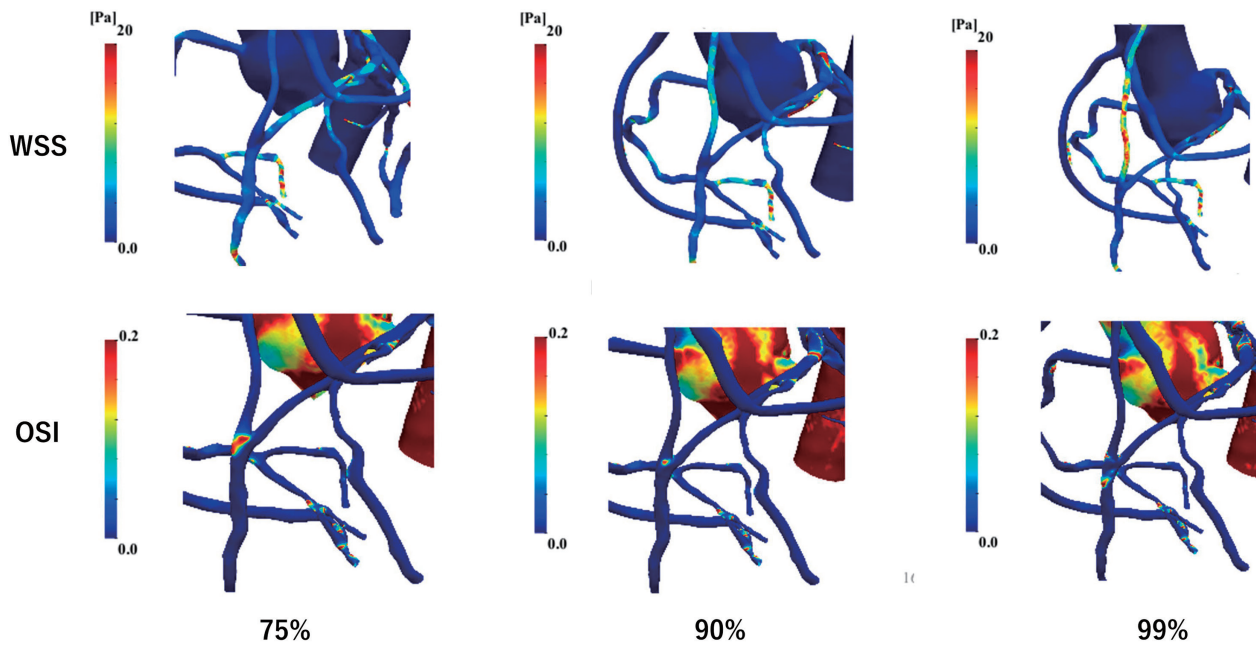


Fig. 2 The WSS at the LAD anastomosis was the highest of the other models and the OSI at the LAD anastomosis was the lowest of the three in the 99% stenosis model. WSS: wall shear stress; LAD: left anterior descending artery; OSI: oscillatory shear index

used to analyze the blood flow to CABG from many angles, and the evaluation of blood flow at the anastomosis and its relationship to WSS and OSI has become clearer.

Ding et al.¹⁴⁾ concluded that, based on the comparisons of time-averaged WSS and OSI, CABG is preferable when the LAD stenosis is higher than 75%. In this study, the stenosis of the native coronary artery was modelled as 0%, 30%, 50%, 75%, and 100%. However, in practice, CABG is not performed below 75%. The study therefore proposed a boundary limit of 75% or more stenosis for bypass, but this is not realistic. Furthermore, this study did not assess the potential of the LITA only by evaluating the anastomosis. The evaluation of the potential of LITA has to take the characteristics of the graft into account. One of the reasons for this is that the LITA has an elastic artery, which is not a characteristic of other grafts.¹⁵⁾ To the best of our knowledge, this study is the first to assess the potential of LITA.

Shimizu et al.¹⁶⁾ investigated the stenosis rate of native vessels with a 75% boundary, and showed that ITAs have higher shear stress than saphenous vein grafts and gastroepiploic artery grafts and may have the adaptive capacity to regulate the vasculature to maintain flow.

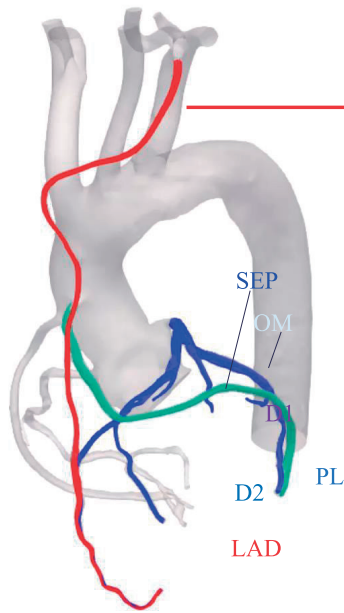
The present study also supports this result. The 99% stenosis model showed the greatest variability in ITA flow velocity, suggesting autoregulation to maintain coronary blood flow and suggesting a large ITA reserve. There is no doubt that this reserve capacity may

contribute to the high patency of ITA. It has been reported that the other reason for the higher patency of ITA is a high production of nitric oxide in ITA compared to other grafts. A high nitric oxide production capacity means a high vasodilatory capacity and a high resistance to atherosclerosis. Future studies are expected to investigate the relationship between these CFD-based studies and endothelium-protective substances such as nitric oxide.

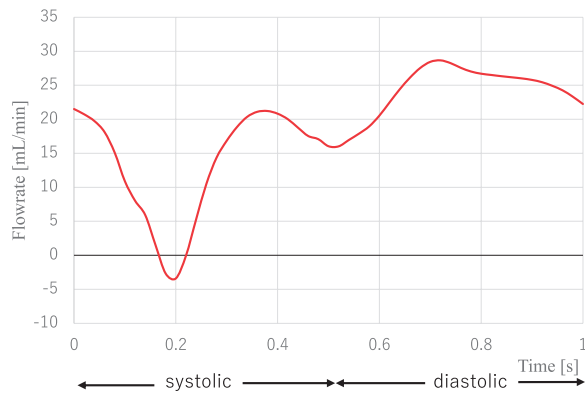
In order to reduce the influence of the anastomosis in ITA graft evaluation, we selected the case that CFD showed to have the least influence on the anastomosis from four cases in this study. The bypass anastomosis method was side-to-side anastomosis in all cases, but the anastomosis method is a factor that can never be ignored as it affects the ITA blood flow velocity. Kanzaki et al. reported that there was no significant difference in bypass blood flow between end-to-side anastomosis and side-to-side anastomosis using CFD.¹⁷⁾

In this study, all anastomoses were performed by side-to-side anastomosis, and Case 2 was selected because of its favorable OSI and TTFM values. By selecting the case with the most stable anastomotic conditions, it was possible to remove the bias due to anastomotic factors. In addition, an *in vitro* model case was designed based on this case to establish the virtual stenosis in the native coronary artery under the same anastomosis conditions, which may have increased the accuracy of this study. Ding et al.¹⁴⁾ mentioned that CABG is preferable for

a Flowrate (LITA anastomosis)

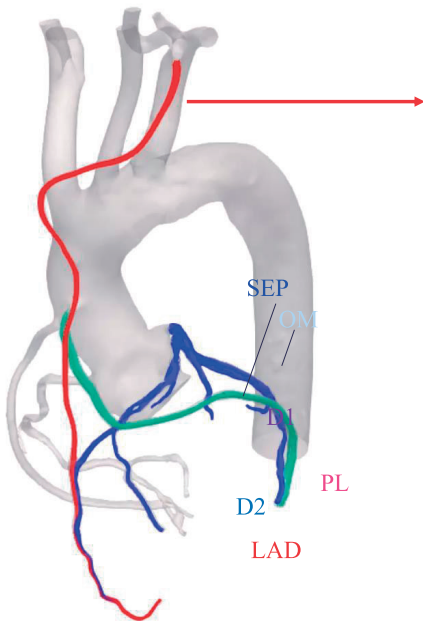


Post CABG Native 75% Stenosis

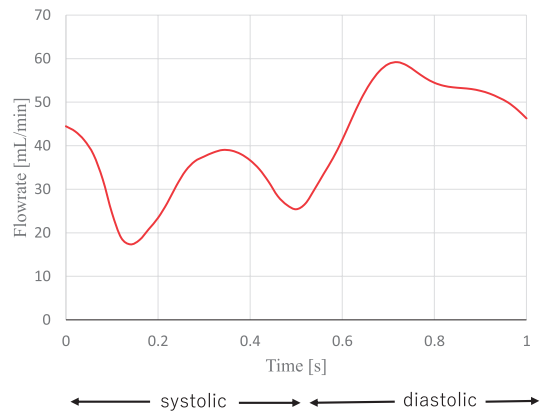


LITA Average Flowrate: 18.9 mL/min

b Flowrate (LITA anastomosis)



Post CABG Native 90% Stenosis



LITA Average Flowrate: 40.4 mL/min

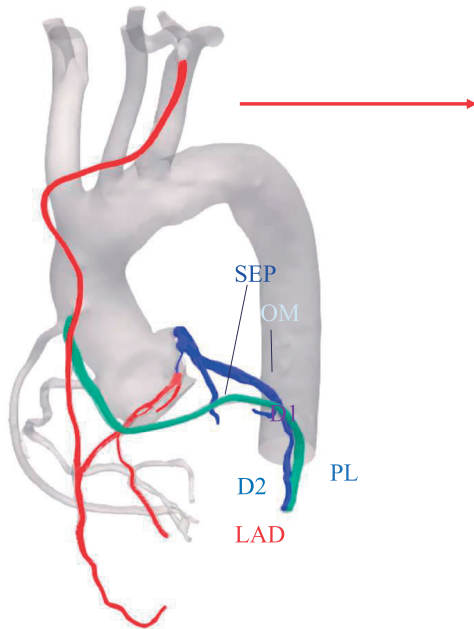
Fig. 3 (Continued)

75% stenosis or more of the target coronary artery. At 75% stenosis, there was a reverse flow from the native coronary artery to the LITA at 0.2 s systole. This regurgitation is commonly referred to as a to-and-fro pattern¹⁸⁾ or a swinging pattern,¹⁹⁾ and is one of the reasons why graft patency can be maintained even at 75% native

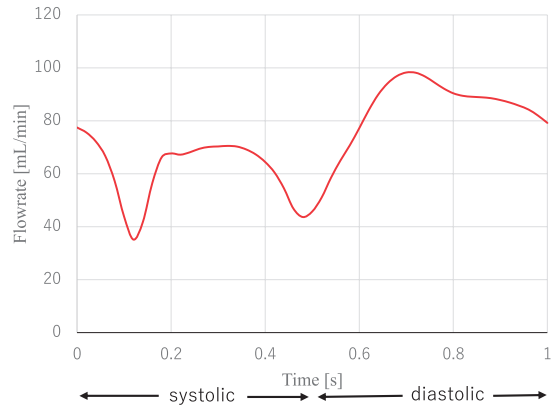
coronary artery stenosis, which should cause stenosis due to the strong anastomotic flow competition compared to 90% or 99% native coronary artery stenosis.¹⁶⁾

In the future, it is expected that further simulation models will be designed and that various findings will be obtained through CFD analysis, such as the evaluation of

c Flowrate (LITA anastomosis)



Post CABG Native 99% Stenosis



LITA Average Flowrate: 72.9 mL/min

Fig. 3 (a) Post CABG native 75% stenosis. (b) Post CABG native 90% stenosis. (c) Post CABG native 99% stenosis. LITA flow rate. In the 99% stenosis model, blood flow from the LITA graft was significantly dominant compared to native coronary flow at the proximal site of anastomosis. LAD: left anterior descending artery; PL: posterolateral branch; OM: obtuse marginal branch; D1: diagnosis 1; D2: diagnosis 2; LITA: left internal thoracic artery; CABG: coronary artery bypass grafting; SEP: septal branch

Table 2 Blood flow in LITA showed a significant increase to 72.9 ml in the 99% model

Area	75%	90%	99%	Stenosis
LAD	66.9	62.6	54.4	
D1	38.8	38.9	39.1	
D2	12.5	11.2	9.14	
SEP	29.6	26.6	22.1	
LITA				
Average	18.9	40.4	72.9	
Min	-5 (0.2 s)	18 (0.15 s)	28 (0.12 s)	
Max	28 (0.7 s)	59 (0.7 s)	98 (0.7 s)	
Range of variability (ml/min)	33	41	70	

The range of LITA flow variability was the largest at 99% stenosis, with a difference of 70 ml/min. LAD: left anterior descending artery; D1: diagnosis 1; D2: diagnosis 2; SEP: septal branch; LITA: left internal thoracic artery

not only the ITA but also other grafts and variations in anastomotic patterns.

Limitations

First, as mentioned by Kanzaki et al.,¹⁷⁾ the simulation geometry is based on coronary artery CT, so the patient’s

condition and CT scan data may affect the shape of the simulation geometry. In CFD blood flow analysis, geometry and boundary conditions have a very large influence on the results. The difference in the quality of the CT results reflects a difference in the shape of the vessel geometry. We believe that this limitation of the CT images may also be responsible for the error between the TTFM values measured intraoperatively and the CFD.

We used 0.625-mm slices during CT to create the geometry and mesh as accurately as possible. The small vessel diameter in a stenotic region cannot always be fully detected on CT images.

Second, simulations using virtual geometry were performed only in one case with the best LITA–LAD anastomosis. The advantage of this virtual geometry simulation based on real patient geometry is that all of the conditions, including vessel geometry shape, aortic pressure, and peripheral resistance, are the same, which enables control experiments using realistic patient geometry. In this way, we can observe the effect of LITA bypass and stenosis severity on blood flow free from other factors. However, the cost of the calculation for each virtual geometry is too high to perform in a large cohort. We would like to find a more cost-effective method in the future to overcome this limitation.

Conclusion

OSI showed no significant change from 75% to 99%. Coronary blood flow was highest at 75% stenosis when LAD, D1, D2, and SEP blood flow were considered. The 99% stenosis model showed the highest LITA flow and compensated for the native coronary artery blood flow. The range of LITA flow variability is large, suggesting that it may vary according to the rate of stenosis of the native coronary artery.

Author Contributions

- (I) Conception and design: K Nakamura, T Nakajima, S Miyazaki, and T Kuniyama
- (II) Administrative support: M Nakao and M Wakatabe
- (III) Provision of study materials or patients: K Nakamura and S Miyazaki
- (IV) Collection and assembly of data: K Nakamura, S Miyazaki, and K Suzuki
- (V) Data analysis and interpretation: K Nakamura, S Miyazaki, and K Suzuki
- (VI) Manuscript writing: K Nakamura
- (VII) Final approval of manuscript: All authors

Declarations

This study was registered with the University Hospital Medical Information Network (study ID: UMIN000045274).

IRB

This study was approved by the IRB of the Saitama Cardiovascular and Respiratory Center (No. 2021009), approval date: 10 May 2021.

Ethics approval and consent to participate

The authors are accountable for all aspects of the work in ensuring that questions related to the accuracy or integrity of any part of the work are appropriately investigated and resolved. This study conformed to the provisions of the Declaration of Helsinki (as revised in 2013). This study was approved by the IRB of the Saitama Cardiovascular and Respiratory Center (No. 2021009).

Consent for publication

Written informed consent was obtained from the patients for using the data for academic publication purposes.

Availability of data and materials

The datasets generated and/or analyzed during the current study are not publicly available due to the possibility that individuals may be identified, but they are available from the corresponding author on reasonable request.

Disclosure Statement

The authors declare that there are no conflicts of interest.

References

- 1) Lytle BW, Blackstone EH, Sabik JF, et al. The effect of bilateral internal thoracic artery grafting on survival during 20 postoperative years. *Ann Thorac Surg* 2004; **78**: 2005–12; discussion, 2012–4.
- 2) Hueb W, Lopes N, Gersh BJ, et al. Ten-year follow-up survival of the Medicine, Angioplasty, or Surgery Study (MASS II): a randomized controlled clinical trial of 3 therapeutic strategies for multivessel coronary artery disease. *Circulation* 2010; **122**: 949–57.
- 3) Nordgaard H, Nordhaug D, Kirkeby-Garstad I, et al. Different graft flow patterns due to competitive flow or stenosis in the coronary anastomosis assessed by transit-time flowmetry in a porcine model. *Eur J Cardiothorac Surg* 2009; **36**: 137–42; discussion, 142.
- 4) Nwasokwa ON. Coronary artery bypass graft disease. *Ann Intern Med* 1995; **123**: 528–45.
- 5) Sabik JF 3rd, Blackstone EH. Coronary artery bypass graft patency and competitive flow. *J Am Coll Cardiol* 2008; **51**: 126–8.
- 6) Villareal RP, Mathur VS. The string phenomenon. An important cause of internal mammary artery graft failure. *Tex Heart Inst J* 2000; **27**: 346–9.
- 7) Nordgaard H, Swillens A, Nordhaug D, et al. Impact of competitive flow on wall shear stress in coronary surgery: computational fluid dynamics of a LIMA-LAD model. *Cardiovasc Res* 2010; **88**: 512–9.
- 8) Berger A, MacCarthy PA, Siebert U, et al. Long-term patency of internal mammary artery bypass grafts; relationship with preoperative severity of the native coronary artery stenosis. *Circulation* 2004; **110**(Suppl 1): II–36–40.
- 9) Itatani K, Miyazaki S, Furusawa T, et al. New imaging tools in cardiovascular medicine: computational fluid dynamics and 4D flow MRI. *Gen Thorac Cardiovasc Surg* 2017; **65**: 611–21.
- 10) Frauenfelder T, Lotfey M, Boehm T, et al. Computational fluid dynamics: hemodynamic changes in abdominal aortic aneurysm after stent-graft implantation. *Cardiovasc Intervent Radiol* 2006; **29**: 613–23.
- 11) Kim KB, Kang CH, Lim C. Prediction of graft flow impairment by intraoperative transit time flow

- measurement in off-pump coronary artery bypass using arterial grafts. *Ann Thorac Surg* 2005; **80**: 594–8.
- 12) Locker C, Mohr R, Lev-Ran O, et al. Comparison of bilateral thoracic artery grafting with percutaneous coronary interventions in diabetic patients. *Ann Thorac Surg* 2004; **78**: 471–5; discussion, 476.
 - 13) Lytle BW, Loop FD, Cosgrove DM, et al. Long-term (5 to 12 years) serial studies of internal mammary artery and saphenous vein coronary bypass grafts. *J Thorac Cardiovasc Surg* 1985; **89**: 248–58.
 - 14) Ding J, Liu Y, Wang F, et al. Impact of competitive flow on hemodynamics in coronary surgery: numerical study of ITA-LAD model. *Comput Math Methods Med* 2012; **2012**: 356187.
 - 15) van Son JA, Smedts F, Vincent JG, et al. Comparative anatomic studies of various arterial conduits for myocardial revascularization. *J Thorac Cardiovasc Surg* 1990; **99**: 703–7.
 - 16) Shimizu T, Ito S, Kikuchi Y, et al. Arterial conduit shear stress following bypass grafting for intermediate coronary artery stenosis: a comparative study with saphenous vein grafts. *Eur J Cardiothorac Surg* 2004; **25**: 578–84.
 - 17) Kanzaki T, Numata S, Yamazaki S, et al. Computational fluid dynamics of internal mammary artery-left anterior descending artery anastomoses. *Interact Cardiovasc Thorac Surg* 2020; **31**: 611–7.
 - 18) Akasaka T, Yoshida K, Hozumi T, et al. Flow dynamics of angiographically no-flow patent internal mammary artery grafts. *J Am Coll Cardiol* 1998; **31**: 1049–56.
 - 19) Shimizu T, Hirayama T, Suesada H, et al. Effect of flow competition on internal thoracic artery graft: postoperative velocimetric and angiographic study. *J Thorac Cardiovasc Surg* 2000; **120**: 459–65.